Proceedings of the 2009 IEEE International Conference on Systems, Man, and Cybernetics
San Antonio, TX, USA - October 2009

# The Design of Internal Type-2 Fuzzy Kinematic Control and Interval Type-2 Fuzzy Terminal Sliding-Mode Dynamic Control of the Wheeled Mobile Robot

*Ming-Ying Hsiao**
*Department of Electrical Engineering*
Fortune Institute of Technology
Kaohsiung, Taiwan 83160, R.O.C.
myhsiao@center.fotech.edu.tw

*Shun-Hung Tsai*
*Graduate Institute of Automation Technology*
National Taipei University of Technology
Taipei, Taiwan 10608, R.O.C.
shtsai@ntut.edu.tw

*Tzuu-Hseng S. Li, Kai-Shiuan. Shih and Chan-Hong Chao*
*Department of Electrical Engineering*
National Cheng Kung University
Tainan, Taiwan 701, R.O.C.
thsli@mail.ncku.edu.tw
n2894115@mail.ncku.edu.tw
n2890109@mail.ncku.edu.tw

*Chi-Hua Liu*
*General Education Center.*
*Fortune Institute of Technology*
*Kaohsiung, Taiwan 83160, R.O.C.*
chliu@center.fotech.edu.tw

***Abstract*—In this paper, a combined intelligent technique is introduced for the trajectory tracking control of a nonholonomic wheeled mobile robot (WMR), which comprises an interval type-2 fuzzy kinematic control (IT2-FKC) and an interval type-2 fuzzy terminal sliding-mode dynamic control (IT2-FTSMDC). Firstly, an interval type-2 fuzzy logic controller designed for the kinematic model of the WMR is introduced, and then the IT2-FTSMDC is developed for the dynamic model of the WMR, which is a combination of the interval type-2 fuzzy logic control (IT2-FLC) and the terminal sliding-mode dynamic control (TSMDC). The validity of the proposed method is demonstrated via computer simulations. The simulation results show that the tracking performance of the IT2-FTSMDC is better than that of the FTSMDC.**

***Keywords—dynamic control, terminal sliding mode, type-2 fuzzy set, type-2 fuzzy logic cobtrol***

## I. INTRODUCTION

Controlling the nonholonomic WMR has been studied widely in recent years [1-5]. Adopting the dynamic model [2-3, 5] is more realistic than just using the kinematic model [1, 4] for the real trajectory tracking control of WMRs. Several of studies have focused on the dynamic model by applying fuzzy-net control [6], sliding-mode control (SMC) [5], back-stepping control [7], and adaptive control [2] to WMRs.

The fuzzy logic control (FLC) has been successfully applied in diverse fields since Zadeh [8] first introduced the fuzzy set theory. Basically, one of the most widely adopted FLCs is rule-based system which is based on human expertise and knowledge. The concept of type-2 fuzzy sets (T2-FSs) [9] is an extension of the well-known ordinary fuzzy sets, the type-1 fuzzy sets (T1-FSs). The membership functions of T2-FSs are three dimensional and include a footprint of uncertainty (FOU), which is a new third dimension of T2-FSs and makes it possible to handle uncertainties [10]. If their secondary membership functions are set to 1, then they are called as the interval type-2 fuzzy sets (IT2-FSs). The architecture of the IT2-FLC is very similar to that of the FLC which contains fuzzifier, rule base, fuzzy inference engine, type-reducer, and defuzzifier. IT2-FLCc can provide more robustness than the conventional FLC to handle the uncertainty and disturbance [11-13].

SMC techniques [5, 14] provide discontinuous control laws to drive the system states to a specified sliding surface and to keep them on the sliding surface. The dynamic performance of the SMC has been adopted as an effective robust control approach for the problems of system uncertainties and external disturbances. To achieve better error convergence property, the parameters of sliding surface must be selected such that the poles of the sliding dynamics should be far away from the origin on the left-half s-plane resulting to increase the gain of the controller. The FSMC [15-16], a hybrid of the SMC and FLC, gives a simple way to design the controller systematically and provides the asymptotical stability of the system. In general, the FSMC can also reduce the rule number in the FLC and still possess robustness.

The terminal sliding-mode (TSM) concept first introduced in [17] can be described as

$$s = \dot{e} + \beta e^{q/p} \tag{1}$$

It has been shown in Zak [18], [19] that $e = 0$ is the terminal attractor of the system $\dot{e} = -\beta e^{q/p}$ .If the initial value $e(0) \neq 0$ and the two odd integers $p$ and $q$ are selected with the condition $p > q$ , then, the relaxation time will be expressed as

$$t_s = \frac{\left|e(0)\right|^{(1-q/p)}}{\beta(1-q/p)} \tag{2}$$

which means that, in the terminal sliding mode, the error state $e$ converges to zero in finite time $t_s$ and the error rate state $\dot{e}$ also converges to zero in finite time identically.

In this paper, a novel interval type-2 fuzzy terminal sliding mode controller is proposed for MWR, which combines the interval type-2 fuzzy logic controller and the terminal sliding mode controller. There are several advantages of the proposed control scheme which can eliminate the chattering phenomena and the system tracking errors converge to zero in finite time.

This paper is organized as follows. In Section II, the kinematic model of the WMR is introduced and an IT2FLC is designed for the WMR. For the dynamic model of the WMR, the design procedure of the IT2-FTSMDC is addressed in detail in Section III. Computer simulation results of the proposed scheme are given in Section IV. Finally, the conclusions are drawn in Section V.

## II. Design The Fuzzy Kinematic Control of the WMR

Firstly, we establish the kinematic model of the WMR in world and robot coordinates, and then an interval type-2 fuzzy controller is designed for the kinematic control of the WMR.

### *A. Kinematic model of the WMR*

Fig. 1 shows the nonholonomic mechanical system of the three-wheel WMR with two driving wheels and a passive wheel. The posture of the WMR can be represented as:

$$\boldsymbol{q} = [x \quad y \quad \theta]^T \tag{3}$$

where the $(x, y)$ is the center of mass (COM) position of the WMR in the world X-Y coordinate, and $\theta$ is the included angle between the X-axis and $X_c$-axis representing the heading of the WMR.

The kinematic model of the WMR can be established by a transformation matrix $\boldsymbol{J}(\theta)$ transforming the velocity $\boldsymbol{v}$ in mobile coordinates to the velocity $\dot{\boldsymbol{q}}$ in Cartesian coordinates as:

$$\dot{\boldsymbol{q}} = \boldsymbol{J}(\theta) \cdot \boldsymbol{v} \tag{4}$$

where $\dot{\boldsymbol{q}} = [\dot{x} \quad \dot{y} \quad \dot{\theta}]^T$, $\boldsymbol{J}(\theta) = \begin{bmatrix} \cos\theta & \sin\theta & 0 \\ 0 & 0 & 1 \end{bmatrix}^T$, $\boldsymbol{v} = [v(t) \quad \omega(t)]^T = [v_1(t) \quad v_2(t)]^T$. The terms $v(t)$ and $\omega(t)$ denote the linear and angular velocities the COM of the WMR,

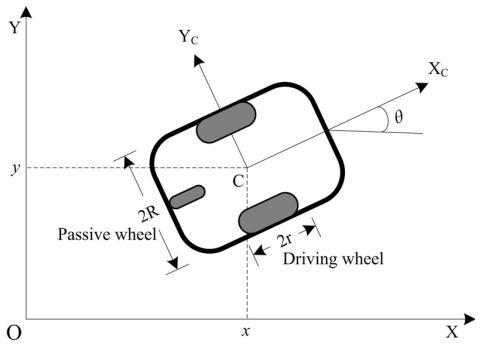


Fig. 1. A nonholonomic WMR with 2 driving wheels and a passive wheel.

respectively. The nonholonomic constraint of the WMR can be expressed as:

$$\dot{y}\cos\theta - \dot{x}\sin\theta = 0 \tag{5}$$

For the trajectory tracking control issue, a reference mobile robot model is given as:

$$\dot{\boldsymbol{q}}_r = \boldsymbol{J}(\theta_r)\boldsymbol{v}_r \tag{6}$$

where $\boldsymbol{v}_r(t)$ and $\boldsymbol{q}_r(t)$ denote the reference velocity and posture of the WMR, respectively. The difference between the desired and actual postures is defined as

$$\boldsymbol{q}_d = \boldsymbol{q}_r - \boldsymbol{q} = \begin{bmatrix} x_e \\ y_e \\ \theta_e \end{bmatrix} = \begin{bmatrix} x_r - x \\ y_r - y \\ \theta_r - \theta \end{bmatrix} \tag{7}$$

With the coordinate transformation $\boldsymbol{T}$, the posture tracking error $\boldsymbol{q}_e$ is defined as :

$$\begin{aligned} \boldsymbol{q}_e &= \begin{bmatrix} e_1 \\ e_2 \\ e_3 \end{bmatrix} = \begin{bmatrix} \cos\theta & \sin\theta & 0 \\ -\sin\theta & \cos\theta & 0 \\ 0 & 0 & 1 \end{bmatrix} \begin{bmatrix} x_r - x \\ y_r - y \\ \theta_r - \theta \end{bmatrix} \\ &= \boldsymbol{T}(\boldsymbol{q}_r - \boldsymbol{q}) = \boldsymbol{T}\boldsymbol{q}_d \end{aligned} \tag{8}$$

Considering the nonholonomic constraint (5), the time derivative of the posture tracking error can be expressed as

$$\dot{\boldsymbol{q}}_e = \begin{bmatrix} \dot{e}_1 \\ \dot{e}_2 \\ \dot{e}_3 \end{bmatrix} = v \begin{bmatrix} -1 \\ 0 \\ 0 \end{bmatrix} + \omega \begin{bmatrix} e_2 \\ -e_1 \\ -1 \end{bmatrix} + \begin{bmatrix} v_r \cos e_3 \\ v_r \sin e_3 \\ \omega_r \end{bmatrix} \tag{9}$$

### *B. Interval type-2 fuzzy kinematic control of the WMR*

The proposed fuzzy kinematic control for the WMR is shown in Fig. 2 at the next page(enclosed by double-dot dashed line).

Some basic concepts of IT2FS are reviewed here. An IT2-FS $\tilde{A}$ is characterized as

$$\tilde{A} = \int_{x \in X} \int_{u \in J_x \subseteq [0,1]} 1/(x,u) = \int_{x \in X} \left[ \int_{u \in J_x \subseteq [0,1]} 1/u \right] \Big/ x \tag{10}$$

where $x \in X$ is the primary variable, $u \in J_x$ is the secondary variable, $J_x \subseteq [0,1]$ is the primary membership of $x$. The secondary grades of $\tilde{A}$ are all equal to 1.

Uncertainty about $\tilde{A}$ can be expressed by the union of all the primary memberships, which is called the footprint of uncertainty (FOU) of $\tilde{A}$ :

$$FOU(\tilde{A}) = \bigcup_{\forall x \in X} J_x = \left\{ (x,u) : u \in \left[ \underline{\mu}_{\tilde{A}}(x), \overline{\mu}_{\tilde{A}}(x) \right] \right\} \tag{11}$$

where $\overline{\mu}_{\tilde{A}}(x) \equiv \overline{FOU(\tilde{A})}$ is the upper bound of FOU and $\underline{\mu}_{\tilde{A}}(x) \equiv \underline{FOU(\tilde{A})}$ is the lower bound of FOU, $\forall x \in X$.

The IT2-FLC controlled system contains the following five components: fuzzifier, rule base, fuzzy inference engine, type-reducer, and defuzzifier.

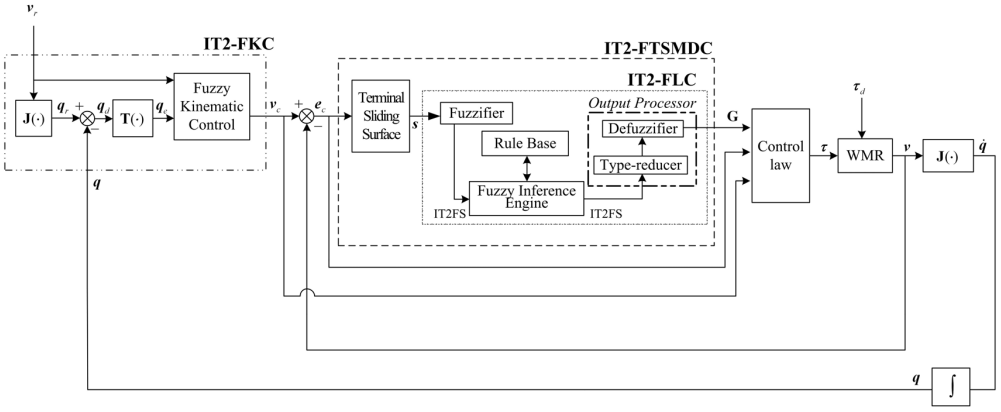


Fig. 2. The complete architect of the IT2-FKC and IT2-FTSMDC for a nonholonomic WMR.

*1) Fuzzifier:*

The fuzzifier maps the singleton value into an interval type-2 fuzzy set. The error $e$ and error rate $\dot{e}$ are considered as the inputs of the diagonal type FLC [20]. We select triangular-shape membership function and the associated upper bound of this membership function with uncertain width, as shown in Fig. 3, which can be expressed as

$$\overline{\mu}_{\tilde{A}}(x)=\begin{cases}0, & x<l_1\\ \dfrac{x-l_1}{p_1-l_1}, & l_1\le x<p_1\\ 1, & p_1\le x\le p_2\\ \dfrac{r_2-x}{r_2-p_2}, & p_2<x\le r_2\\ 0, & x>r_2\end{cases} \tag{12a}$$

and the corresponding lower bound MF is

$$\underline{\mu}_{\tilde{A}}(x)=\begin{cases}0, & x<l_2\\ \dfrac{x-l_2}{p_2-l_2}, & x\le \dfrac{r_1(p_2-l_2)+l_2(r_1-p_1)}{(p_2-l_2)+(r_1-p_1)}\\ \dfrac{r_1-x}{r_1-p_1}, & x>\dfrac{r_1(p_2-l_2)+l_2(r_1-p_1)}{(p_2-l_2)+(r_1-p_1)}\\ 0, & x>r_1\end{cases} \tag{12b}$$

*2) Rule base:*

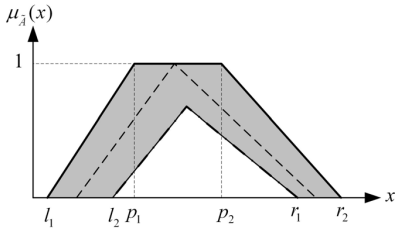


Fig. 3. A triangular-shape IT2FS is with its principal T1FS (dot line), bounded by an upper bound MF (thicker solid line) and a lower bound MF (thicker dot-dashed line).

The rules for IT2-FLC are similar to those for the conventional type-1 FLC in the IF-THEN form. The $i$-th rule for the IT2-FLC can be written as

$$R^i:\ \text{IF } e_1 \text{ is } \tilde{F}_{i1} \text{ and } e_2 \text{ is } \tilde{F}_{i2}$$
$$\text{THEN } u \text{ is } \tilde{G}_i \quad i=1,\ldots,M \tag{13}$$

where the IT2-FSs $\tilde{F}_{i1},\tilde{F}_{i2}\subseteq[NE_n\cdots NE_1\ ZE\ PO_1\cdots PO_n]$ and $\tilde{G}_i\subseteq[NE_m\cdots NE_1\ ZE\ PO_1\cdots PO_m]$. $NE_i$ and $PO_i$ denote the $i$-th negative and positive IT2-MFs, respectively. Here we choose the diagonal-type rule table due to the similarity between the diagonal type FLC and SMC [20]. The rule table of the diagonal IT2-FLC is listed in Table I.

*3) Fuzzy inference engine:*

The inference engine combines all the fired rules and gives a nonlinear mapping from the input IT2-FSs to the output IT2-FSs. The multiple antecedents in each rule are connected by using the Meet operation, the membership grades in the input

TABLE I
DIAGONAL-TYPE RULE TABLE FOR IT2-FLC

| $u$ \ $e$ / $\dot{e}$ | $NE_n$ | $NE_{n-1}$ | … | $NE_1$ | ZE | $PO_1$ | … | $PO_{n-1}$ | $PO_n$ |
|---|---|---|---|---|---|---|---|---|---|
| $PO_n$ | ZE | $PO_1$ | | | | | | $PO_{m-1}$ | $PO_m$ |
| $PO_{n-1}$ | $NE_1$ | ZE | $PO_1$ | | | | | | $PO_{m-1}$ |
| ⋮ | | $NE_1$ | ZE | $PO_1$ | | | ⋱ | | |
| $PO_1$ | | | $NE_1$ | ZE | $PO_1$ | | | | |
| ZE | | | | $NE_1$ | ZE | $PO_1$ | | | |
| $NE_1$ | | | | | $NE_1$ | ZE | $PO_1$ | | |
| ⋮ | | | ⋰ | | | $NE_1$ | ZE | $PO_1$ | |
| $NE_{n-1}$ | $NE_{m-1}$ | | | | | | $NE_1$ | ZE | $PO_1$ |
| $NE_n$ | $NE_m$ | $NE_{m-1}$ | | | | | | $NE_1$ | ZE |

sets are combined with those in the output sets by using the extended sup-star composition as:

$$\mu_{R^l}(\boldsymbol{e},u) = \sqcap_{i=1}^{p} \mu_{\tilde{F}_i^l}(e_i) \sqcap \mu_{\tilde{G}^l}(u) \tag{14}$$

where $\sqcap$ denotes the Meet operation, $p$ is the number of input variables, and $\sqcap_{i=1}^{p} \mu_{\tilde{F}_i^l}(e_i) \equiv \tilde{F}(\boldsymbol{e})$, which results in an interval set described by

$$\tilde{F}(\boldsymbol{e}) = \left[\underline{f}^i(\boldsymbol{e}), \overline{f}^i(\boldsymbol{e})\right] = \left[\underline{f}^i, \overline{f}^i\right] \tag{15}$$

*4) Type reducer:*

The type-reducer is an extension of the type-1 defuzzifier which can be obtained by applying the Extension Principle [9]. It represents a mapping of a T2-FS into a T1-FS. For an IT2-FLC, regardless of the type-reducing method or the membership function of the input variables, the type-reduced set is always an interval set and is determined by its two end points $u_l(\boldsymbol{e})$ and $u_r(\boldsymbol{e})$. The type-reduced set using the center of sets (COS) type-reduction can be expressed as

$$\begin{aligned} U_{\cos}(\boldsymbol{e}) &= [u_l, u_r] \\ &= \int_{u^1 \in \left[u_l^1, u_r^1\right]} \cdots \int_{u^M \in \left[u_l^M, u_r^M\right]} \int_{f^1 \in \left[\underline{f}^1, \overline{f}^1\right]} \cdots \int_{f^M \in \left[\underline{f}^M, \overline{f}^M\right]} 1 \Big/ \frac{\sum_{i=1}^{M} f^i u^i}{\sum_{i=1}^{M} f^i} \end{aligned} \tag{16}$$

where $U_{\cos}(\boldsymbol{e})$ is an interval output set determined by its left-most point $u_l(\boldsymbol{e})$ and its right-most point $u_r(\boldsymbol{e})$. In order to compute $u_l(\boldsymbol{e})$ and $u_r(\boldsymbol{e})$, the Karnik–Mendel iterative procedure is needed [21].

*5) Defuzzifier:*

At the type-reducer, we have a type-reduced set $U_{\cos}(\boldsymbol{e})$ for each output determined by its left-most point $u_l(\boldsymbol{e})$ and right-most point $u_r(\boldsymbol{e})$. The interval set can be defuzzified by using the average of $u_l(\boldsymbol{e})$ and $u_r(\boldsymbol{e})$; hence, the defuzzified crisp output of the IT2-FLC becomes

$$\boldsymbol{v}_c(\boldsymbol{e}) = \frac{u_l(\boldsymbol{e}) + u_r(\boldsymbol{e})}{2} \tag{17}$$

The output of the fuzzy kinematic control $\boldsymbol{v}_c$ will lead the tracking error approaching to zero.

## III. Designing the IT2-FTSMDC for the WMR

The design procedures of the proposed IT2-FTSMDC for the WMR will be described in detail in this section.

### A. Dynamic model of the WMR

The dynamic model of the WMR [3,6] can be expressed as:

$$\boldsymbol{M}(\boldsymbol{q})\ddot{\boldsymbol{q}} + \boldsymbol{V}_m(\boldsymbol{q},\dot{\boldsymbol{q}})\dot{\boldsymbol{q}} + \boldsymbol{F}_{\mathrm{G}}(\boldsymbol{q}) + \boldsymbol{\tau}_d = \boldsymbol{B}(\boldsymbol{q})\boldsymbol{\tau} - \boldsymbol{C}^{\mathrm{T}}(\boldsymbol{q})\boldsymbol{\lambda} \tag{18}$$

where $\boldsymbol{q} \in R^{n\times 1}$ is position vector, $\boldsymbol{M}(\boldsymbol{q}) \in R^{n\times n}$ is a positive symmetric definite inertia matrix, $\boldsymbol{V}_m(\boldsymbol{q},\dot{\boldsymbol{q}}) \in R^{n\times n}$ is the centripetal and Coriolis matrix, $\boldsymbol{F}_{\mathrm{G}}(\boldsymbol{q}) \in R^{n\times 1}$ is the gravitational vector, $\boldsymbol{\tau}_d \in R^{n\times 1}$ is bounded unknown disturbance, $\boldsymbol{B}(\boldsymbol{q}) \in R^{n\times(n-m)}$ is the input transformation matrix, $\boldsymbol{\tau} \in R^{(n-m)\times 1}$ is the control input vector, $\boldsymbol{C} \in R^{m\times n}$ is a matrix associated with the nonholonomic constraints, $\boldsymbol{\lambda} \in R^{m\times 1}$ is a Lagrange multiplier associated with the constraints, and $\dot{\boldsymbol{q}}$ and $\ddot{\boldsymbol{q}}$ denote velocity and acceleration vectors, respectively. The parameters in (16) are given as:

$$\boldsymbol{M}(\boldsymbol{q}) = \begin{bmatrix} m & 0 & 0 \\ 0 & m & 0 \\ 0 & 0 & I \end{bmatrix}, \quad \boldsymbol{B}(\boldsymbol{q}) = \frac{1}{r}\begin{bmatrix} \cos\theta & \cos\theta \\ \sin\theta & \sin\theta \\ R & -R \end{bmatrix}, \quad \boldsymbol{F}_{\mathrm{G}}(\boldsymbol{q}) = 0,$$

$\boldsymbol{\tau}^T = [\tau_r \quad \tau_l]$, and $\boldsymbol{C}(\boldsymbol{q}) = [-\sin\theta \quad \cos\theta \quad 0]$, where $m$ and $I$ are the mass and the moment of inertia of the WMR, respectively. $R$ and $r$ are the distances between the two driving wheels and the radius of the wheel, respectively. $\tau_r$ and $\tau_l$ are torque control inputs generated from the right and left DC motor, respectively.

By Taking the derivative of (4) and substituting it into (18), then pre-multiplying each term by $\boldsymbol{J}^T$, the dynamic equation (18) becomes

$$\bar{\boldsymbol{M}}(\boldsymbol{q})\dot{\boldsymbol{v}} + \bar{\boldsymbol{\tau}}_d = \bar{\boldsymbol{B}}(\boldsymbol{q})\boldsymbol{\tau} \tag{19}$$

where $\bar{\boldsymbol{M}} = \boldsymbol{J}^{\mathrm{T}}\boldsymbol{M}\boldsymbol{J} \in R^{2\times 2}$, $\bar{\boldsymbol{\tau}}_d = \boldsymbol{J}^{\mathrm{T}}\boldsymbol{\tau}_d$, and $\bar{\boldsymbol{B}} = \boldsymbol{J}^{\mathrm{T}}\boldsymbol{B}$.

Without considering uncertainties and disturbances, the nominal dynamic model of (19) becomes

$$\dot{\boldsymbol{v}}(t) = \boldsymbol{E}_0 \cdot \boldsymbol{\tau}(t) \tag{20}$$

where $\boldsymbol{E}_0 = \bar{\boldsymbol{M}}^{-1}(\boldsymbol{q})\bar{\boldsymbol{B}}(\boldsymbol{q})$.

### B. TSMDC design of the WMR

The proposed IT2-FTSMDC scheme for the WMR is shown in Fig. 2 (enclosed by the dashed line). The control purpose of the IT2-FTSMDC is to ensure the actual velocity of the WMR converges to the reference one. Before constructing the IT2-FTSMDC for the WMR system, one must design TSMDC for the nominal system first. We introduce the auxiliary velocity tracking error and its time derivative as

$$\boldsymbol{e}_c(t) = [e_{c1}(t)\ e_{c2}(t)]^{\mathrm{T}} = [v_{c1}(t) - v_1(t) \quad v_{c2}(t) - v_2(t)]^{\mathrm{T}} \tag{21}$$

$$\dot{\boldsymbol{e}}_c(t) = \dot{\boldsymbol{v}}_c(t) - \dot{\boldsymbol{v}}(t) \tag{22}$$

where $i = 1, 2$. The integral type terminal sliding surface is selected as:

$$\boldsymbol{s}(t) = \left[s_1(t) \quad s_2(t)\right]^T = \boldsymbol{e}_c(t) + \boldsymbol{\beta}\int_0^t \boldsymbol{e}_c^{q/p}(\tau)d\tau \tag{23}$$

where $\boldsymbol{\beta} = \begin{bmatrix} \beta_1 & 0 \\ 0 & \beta_2 \end{bmatrix}$, $\beta_i$ is a positive constant and $i = 1, 2$. Furthermore, once the system is on the sliding surface, then, $\boldsymbol{s}(t) = 0$. The time derivative of the sliding surface $\boldsymbol{s}(t)$ becomes

$$\dot{\boldsymbol{s}}(t) = [\dot{\boldsymbol{v}}_c(t) - \dot{\boldsymbol{v}}(t)] + \boldsymbol{\beta}_i \boldsymbol{e}_c^{q/p} \tag{24}$$

The equivalent control law $\boldsymbol{\tau}_{eq}$ for the nominal system is given by

$$\boldsymbol{\tau}_{eq}(t) = \boldsymbol{E}_0^{-1}\left(\dot{\boldsymbol{v}}_c(t) + \boldsymbol{\beta}\boldsymbol{e}_c^{q/p}(t)\right) \tag{25}$$

Unfortunately, disturbances and uncertainties always exist and the discontinuous control law $\boldsymbol{\tau}_{sw}$ will be introduced to tackle them.

Now, the dynamic model (19) with parameter uncertainties and external disturbances can be expressed as:

$$\dot{\boldsymbol{v}}(t) = \boldsymbol{E}\cdot\boldsymbol{\tau}(t) + \overline{\boldsymbol{\tau}}_d = (\boldsymbol{E}_0 + \Delta\boldsymbol{E})\cdot\boldsymbol{\tau}(t) + \overline{\boldsymbol{\tau}}_d \tag{26}$$

where $\boldsymbol{E}_0$ and $\Delta\boldsymbol{E}$ denotes the nominal part and the uncertainty part of system matrix $\boldsymbol{E}$, respectively. $\boldsymbol{\Phi}(t)$ is defined as the sum of these uncertainties and disturbances

$$\boldsymbol{\Phi}(t) = \Delta\boldsymbol{E}\cdot\boldsymbol{\tau}(t) + \overline{\boldsymbol{\tau}}_d \tag{27}$$

where $\boldsymbol{\Phi}(t) = [\phi_1 \quad \phi_2]^T$, $|\phi_i(t)| \le d_i, i = 1,2$, and $d_i$ is a finite positive constant. Then (26) becomes

$$\dot{\boldsymbol{v}}(t) = \boldsymbol{E}_0\cdot\boldsymbol{\tau}(t) + \boldsymbol{\Phi}(t) \tag{28}$$

Now, the control law is composed of $\boldsymbol{\tau}_{eq}$ and $\boldsymbol{\tau}_{sw}$ which can be expressed as

$$\boldsymbol{\tau} = \boldsymbol{\tau}_{eq} + \boldsymbol{\tau}_{sw} = \boldsymbol{E}_0^{-1}\left(\dot{\boldsymbol{v}}_c(t) + \boldsymbol{\beta}\boldsymbol{e}_c^{q/p}(t) + \boldsymbol{\Gamma}\cdot\mathrm{sgn}(\boldsymbol{s})\right) \tag{29}$$

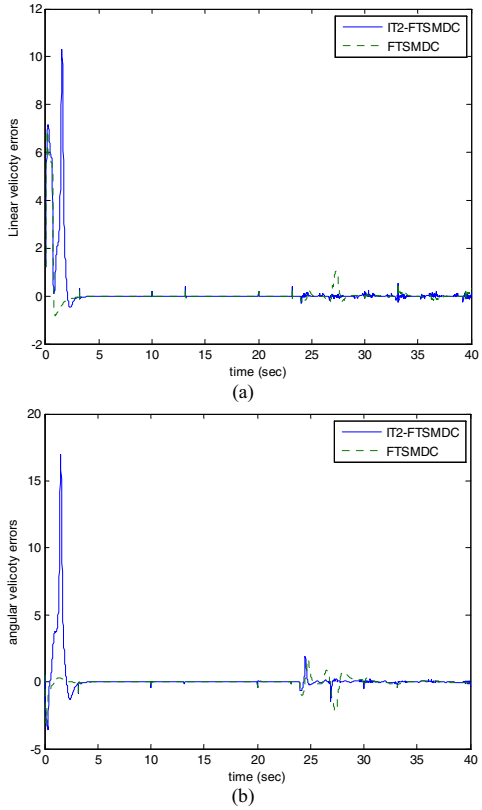


Fig. 5. The round rectangle trajectory-tracking (a) The linear velocity tracking errors of the FTSMDC; (b) The angular velocity tracking errors of the IT2-FTSMDC.

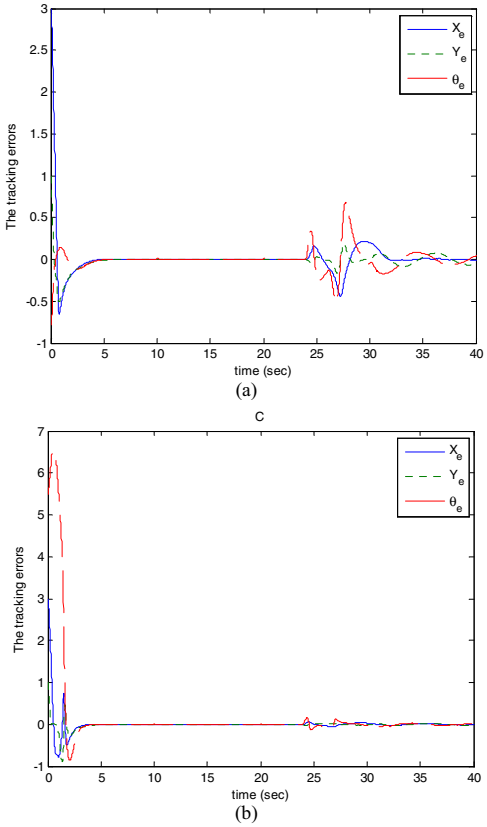


Fig. 4. The round rectangle trajectory-tracking (a) The tracking errors of the FTSMDC; (b) The tracking errors of the IT2-FTSMDC.

where $\boldsymbol{\Gamma} = \begin{bmatrix} \gamma_1 & 0 \\ 0 & \gamma_2 \end{bmatrix}$, and $\gamma_i > 0$, $i = 1,2$.

### C. IT2-FTSMDC design of the WMR

For the IT2-FTSMDC, we select the sliding surface as the inputs of the controlled system. The *i*-th fuzzy rule of the IT2-FSMDC can be expressed as:

$$R^i: \text{IF } s_j \text{ is } \tilde{S}_{ij} \text{ THEN } g_j \text{ is } \tilde{\alpha}_{ij} \quad i = 1,\cdots,M \text{ and } j = 1,2 \tag{30}$$

The switching controller now can be selected as

$$\boldsymbol{\tau}_{sw} = \boldsymbol{E}_0^{-1}\boldsymbol{\Gamma}\mathbf{sgn}(\boldsymbol{s}) = \boldsymbol{G}\mathbf{sgn}(\boldsymbol{s}) \tag{31}$$

where $\boldsymbol{G} = \begin{bmatrix} g_1 & 0 \\ 0 & g_2 \end{bmatrix}$, and $g_j \ge 0$ ($j$ = 1, 2).

## IV. Computer Simulations

Simulations are utilized to examine the feasibility and the validity of the proposed control scheme. A round rectangle trajectory is adopted to test the trajectory-tracking capability of the proposed method. The triangular-shape and singleton-type with three even partitions are chosen as the membership functions of the IF-part and THEN-part in both of the

TABLE II
COMPARISON OF PERFORMANCE OF FTSMDC AND IT2-FTSMDC APPLIED TO WMR FOR TRACKING A DESIRED TRAJECTORY.

| Controller | IAE | ITAE | ISE | ITSE |
|---|---|---|---|---|
| FTSMDC | 446.6 | 5975.3 | 361.4 | 5050.2 |
| IT2-FTSMDC | 328.4 | 2052.3 | 266.6 | 1546.4 |

FTSMDC and the IT2-FTSMDC, respectively. The parameters of the WMR in simulation are selected as $m = 5\text{kg}$ , $I$=3.5kg$\cdot$m$^2$ , $R = 0.25\text{m}$ , and $r = 0.05\text{m}$ .

The initial posture of the reference trajectory is set to $\boldsymbol{q}_r(0) = [5,\ 0,\ 0°]^T$ and initial posture of the WMR is set to $\boldsymbol{q}(0) = [2,\ -1,\ 45°\ ]^T$ .We apply an external disturbances, $\boldsymbol{\tau}_d = 25\sin(t-24)$ to the WMR at $t = 24s$ , and also vary the inertia of the WMR from 3.5 kg$\cdot$m$^2$ to 7 kg$\cdot$m$^2$ at $t = 12s$ .

The trajectory tracking results are shown in Fig. 4. The velocity tracking errors are shown in Fig.5. The performance comparison of FSTMDC and IT2-FSMDC are summarized in Table II, including integral of the absolute error (IAE), the integral of the time multiplied by the absolute value of the error (ITAE), integral of square error (ISE) and integral of the time multiplied by the square error (ITSE). One can find from the figures and table that the IT2-FTSMDC outperforms the FTSMDC.

## V. CONCLUSIONS

We have conducted a thorough study including kinematic and dynamic control designs for the trajectory tracking control of the nonholonomic WMR. The design schemes of the IT2-FKC and the IT2-FTSMDC have been introduced in detail. The simulation results show that, from the IAE, ITAE, ISE, and ITSE points of views, the tracking performance of the IT2-FTSMDC is better than that of the FTSMDC.

## ACKNOWLEDGMENT

This work was supported by the National Science Council of Taiwan, R.O.C., under Grant NSC97-2218-E-027-022.

## REFERENCES

[1] R. Carelli, J. Santos-Victor, F. Roberti, and S. Tosetti, "Direct visual tracking control of remote cellular robots," Robotics and Autonomous Systems, vol. 54, pp. 805–814, 2006.

[2] T. Das, and I. N. Kar, "Design and implementation of an adaptive fuzzy logic-based controller for wheeled mobile robots," IEEE Transactions on Control Systems Technology, vol. 14, pp. 501–510, 2006.

[3] W.-S. Lin, C.-L. Huang, and M.-K. Chuang, "Hierarchical fuzzy control for autonomous navigation of wheeled robots," IEE Proceedings-Control Theory and Applications, vol. 152, pp. 598–606, 2005.

[4] S. Sun, "Designing approach on trajectory-tracking control of mobile robot," Robotics Computer-Integrated Manufacturing, vol. 21, pp. 81–85, 2005.

[5] D. Chwa, "Sliding-mode tracking control of nonholonomic wheeled mobile robots in polar coordinates," IEEE Transactions on Control Systems Technology, vol. 12, pp. 637–644, 2004.

[6] A. V. Topalov, J. H. Kim, and T. P. Proychev, "Fuzzy-net control of non-holonomic mobile robot using evolutionary feedback-error-learning," Robotics and Autonomous Systems, vol. 23, pp. 187–200, 1998.

[7] F. Pourboghrat and M. P. Karlsson, "Adaptive control of dynamic mobile robots with nonholonomic constraints," *Computers and Electrical Engineering, vol.* 28, pp. 241–253, 2002.

[8] L. A. Zadeh, "Fuzzy sets," Information and Control, vol. 8, pp. 338–353, 1965.

[9] L. A. Zadeh, "The concept of a linguistic variable and its application to approximate reasoning—I," Information Sciences, vol. 8, pp. 199–249, 1975.

[10] J. M. Mendel and R. John, "Type-2 fuzzy sets made simple," IEEE Trans. on Fuzzy Systems, vol. 10, pp. 117–127, 2002.

[11] L. Astudillo, O. Castillo, and L. T. Aguilar, "Intelligent control for a perturbed autonomous wheeled mobile robot: A type-2 fuzzy logic approach," Journal of Nonlinear Studies, vol. 14, no. 3, pp. 37–48, 2007.

[12] H. A. Hagras, "A hierarchical type-2 fuzzy logic control architecture for autonomous mobile robots," IEEE Trans. on Fuzzy Systems, vol. 12, no. 4, pp. 524–539, 2004.

[13] M.-Y. Hsiao, T.- H. S. Li, J.-Z. Lee, C.-H. Chao, and S.-H. Tsai, "Design of interval type-2 fuzzy sliding-mode controller," Information Sciences, vol. 178, no. 6, pp. 1696–1716, 2008.

[14] J.-Y. Hung, W. Gao, and J.-C. Hung, "Variable structure control: A survey," IEEE Trans. Indus. Elect. vol. 40, no. 1, pp. 2–22, 1993.

[15] T.-H. S. Li and M.-Y. Shieh, Switching-type fuzzy sliding-mode control of a cart-pole system, Mechatronics, vol. 10, pp. 91–101, 2000.

[16] J. Wang, A. B. Rad, and P.T. Chan, "Indirect adaptive fuzzy sliding-mode control: Part I: Fuzzy switching," Fuzzy Sets and System, vol. 122, pp. 21–30, 2001.

[17] Z. Man, A. P. Paplinski, and H. R. Wu, "A robust MIMO terminal sliding mode control for rigid robotic manipulators," IEEE Trans. Automat. Contr., vol. 39, pp. 2464–2469, Dec. 1994

[18] M. Zak, "Terminal atractors for addressable memory in neural network," Phys. Lett. A, vol. 133, no. 1,2, pp. 18–22, 1988.

[19] M. Zak "Terminal attractors in neural networks," Neural Networks, vol. 2, pp. 259–274, 1989.

[20] S. G. Tzafestas, G. G. Rigatos, "A simple robust sliding-mode fuzzy-logic controller of the diagonal type," Journal of Intelligent and Robotic Systems, vol. 26, pp. 353-388, 1999.

[21] N. N. Karnik and J. M. Mendel, "Centroid of a type-2 fuzzy set," Information Sciences, vol. 132, pp. 195–220, 2001.